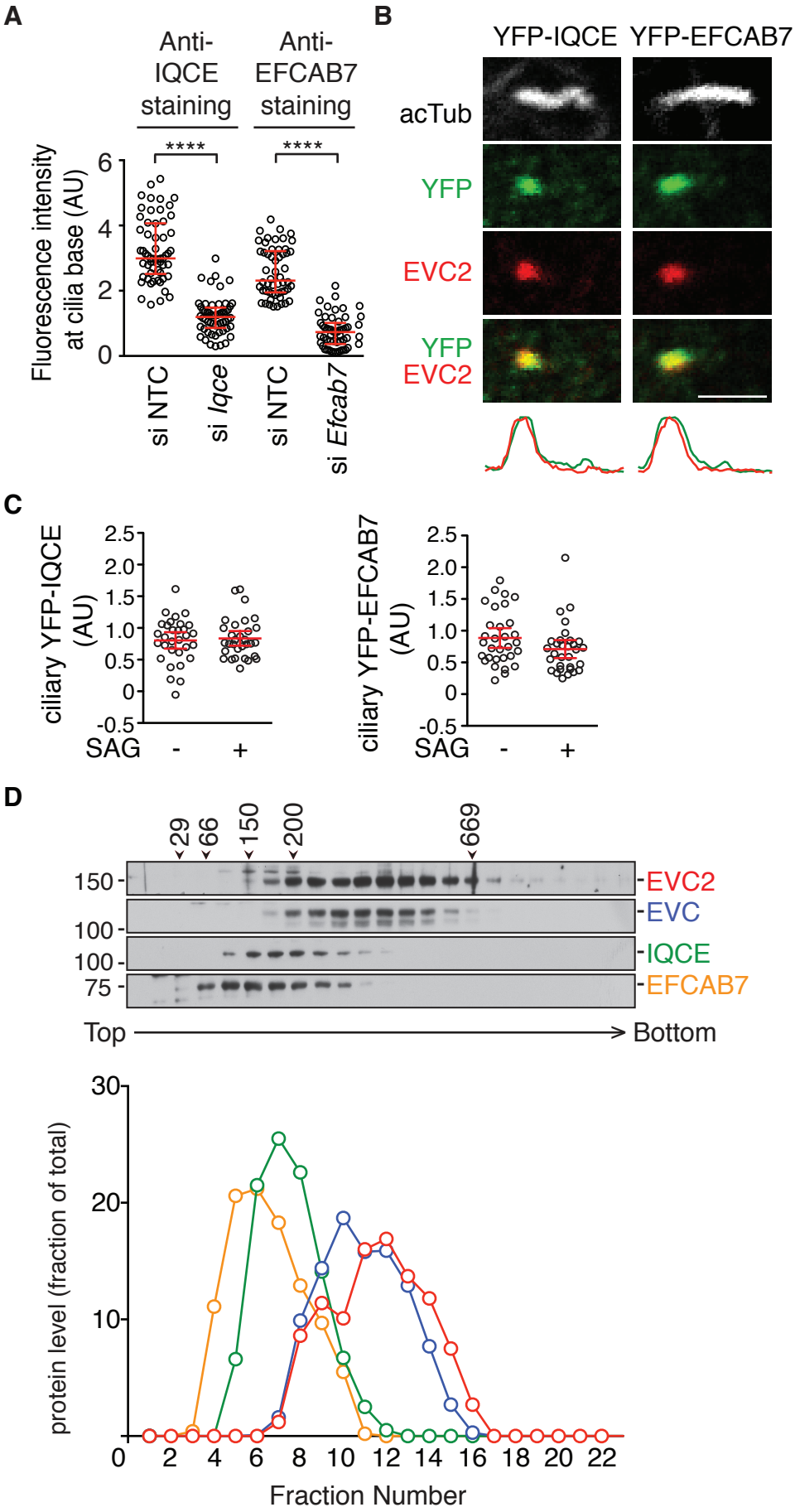
A
Anti-IQCE staining
Anti-EFCAB7 staining
****
****
Fluorescence intensity at cilia base (AU)
si NTC
si Iqce
si NTC
si Efcab7
B
YFP-IQCE
YFP-EFCAB7
acTub
YFP
EVC2
YFP
EVC2
C
ciliary YFP-IQCE (AU)
SAG - +
ciliary YFP-EFCAB7 (AU)
SAG - +
D
29
66
150
200
669
EVC2
EVC
IQCE
EFCAB7
Top
Bottom
protein level (fraction of total)
Fraction Number

Figure S1, related to Figure 1 and Figure 2. The EFCAB7-IQCE complex localizes at the base of primary cilia.

(A) EFCAB7 and IQCE immunostaining at the base of cilia is reduced after siRNA-mediated depletion of the corresponding protein antigen, showing that the anti-IQCE and anti-EFCAB7 rabbit polyclonal antibodies developed in this study are specific. Each point represents staining intensity at the base of a single cilium and the red brackets show median fluorescence and interquartile ranges, with significance established using Kruskal-Wallis test; $p<0.0001$ (****), n=55. (B) YFP-IQCE and YFP-EFCAB7 (green) stably expressed in NIH/3T3 cells co-localize with endogenous EVC2 (red) at the base of primary cilia, oriented with the base to the left and tip to the right and identified with anti-acetylated tubulin staining (white, acTub). Plots below the images indicate normalized fluorescent intensities for each of the channels along the cilium from base (left) to tip (right). Scale bar: 2 μm. (C) The levels of IQCE (left) and EFCAB7 (right) at the base of cilia do not change when the Hh pathway is activated with SAG. Each point represents staining in single cilium and the red lines show the mean (±SD) fluorescence intensities from multiple cilia (n=30). (D) Fractionation of endogenous EvC complex components on a 10-30% (w/w) glycerol gradient. The immunoblot (top) and graph (below) depict the amount protein found in each fraction collected from the gradient. The numbers and arrows above the immunoblots denote the molecular weights (in kDa) and peak elution positions of a set of standard proteins.

Figure S2

ECH1

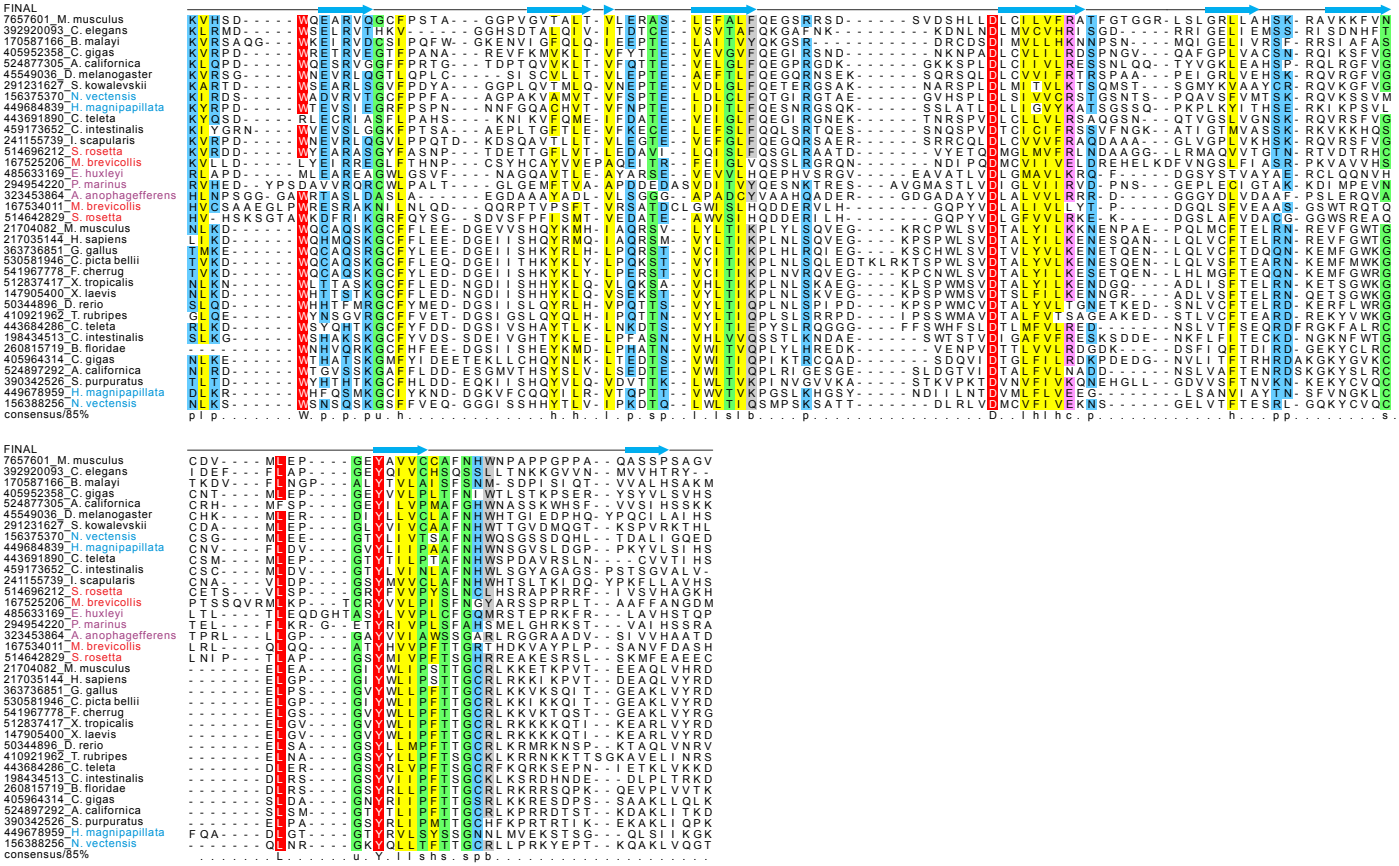

ECH2

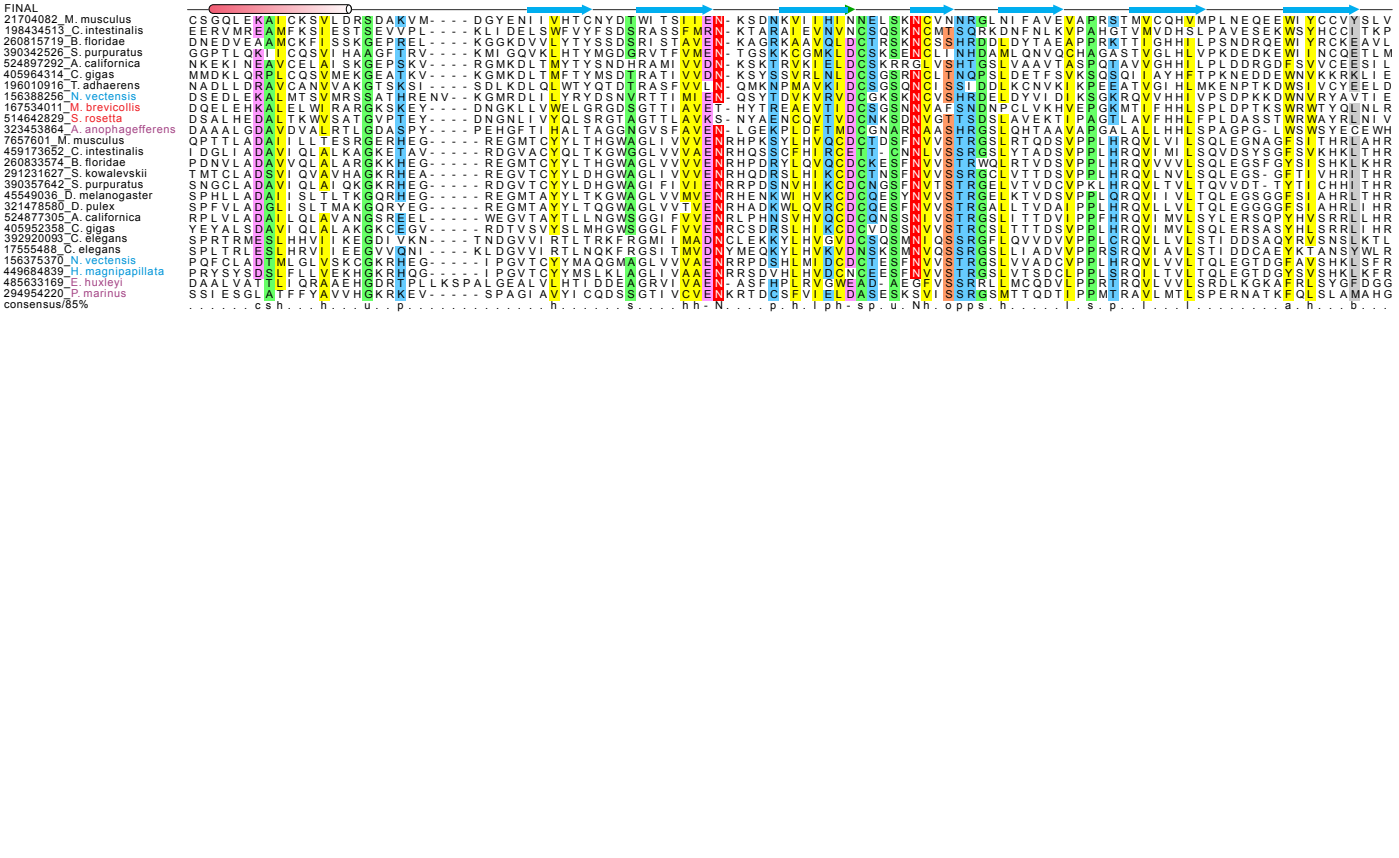

Figure S2, related to Figure 4. Multiple sequence alignments of the ECH1 and ECH2 domains present in EFCAB7 and Calpain-15 proteins.

Predicted secondary structure is denoted above each alignment. Both globular domains are predicted to adopt a β-sandwich fold.

Figure S3

IQCE

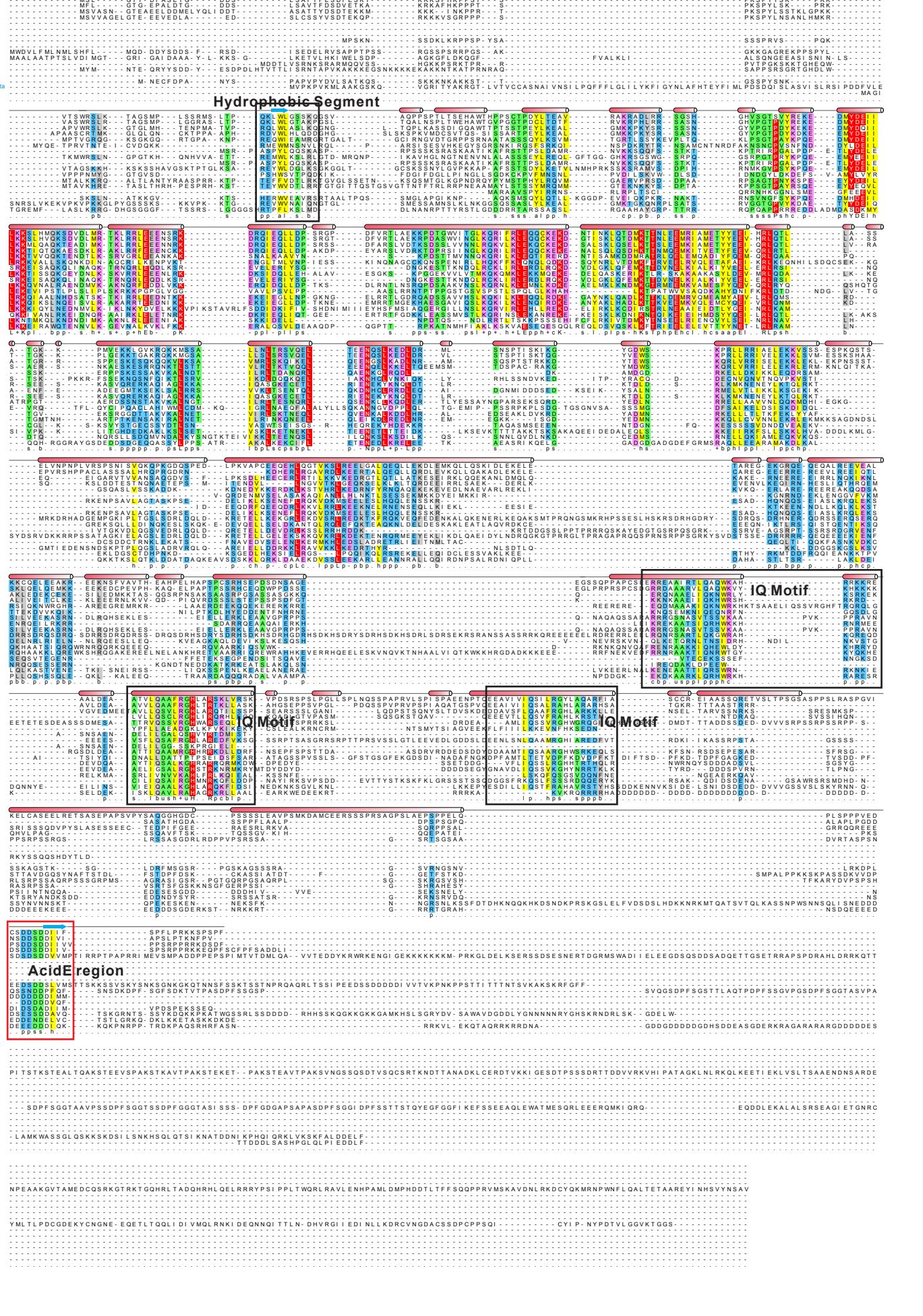

Figure S3, related to Figure 4. Multiple sequence alignment of the IQCE proteins.

Labels denote the hydrophobic segment, three IQ motifs, and AcidE region.

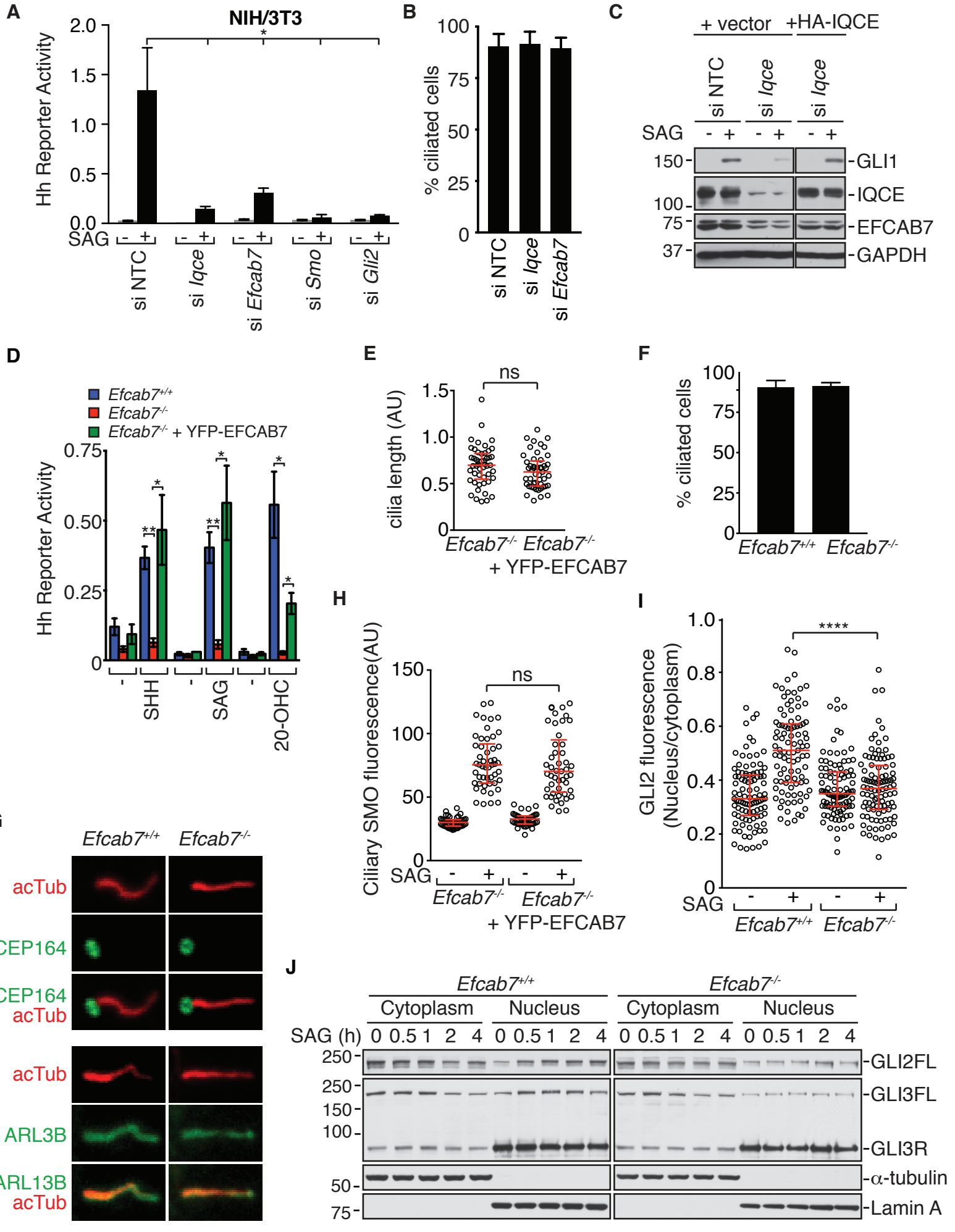
A
NIH/3T3
Hh Reporter Activity
SAG
si NTC
si Ifce
si Efcab7
si Smo
si Gli2
B
% ciliated cells
si NTC
si Ifce
si Efcab7
C
+ vector
+HA-IQCE
si NTC
si Ifce
si Ifce
SAG
GLI1
IQCE
EFCAB7
GAPDH
D
Efcab7+/+
Efcab7-/-
Efcab7-/- + YFP-EFCAB7
Hh Reporter Activity
SHH
SAG
20-OHC
E
cilia length (AU)
ns
Efcab7-/-
Efcab7-/-
+ YFP-EFCAB7
F
% ciliated cells
Efcab7+/+
Efcab7-/-
G
Efcab7+/+
Efcab7-/-
acTub
CEP164
CEP164
acTub
acTub
ARL3B
ARL13B
acTub
H
Ciliary SMO fluorescence(AU)
ns
SAG
Efcab7-/-
Efcab7-/-
+ YFP-EFCAB7
I
GLI2 fluorescence
(Nucleus/cytoplasm)
****
SAG
Efcab7+/+
Efcab7-/-
J
Efcab7+/+
Efcab7-/-
Cytoplasm
Nucleus
SAG (h) 0 0.5 1 2 4 0 0.5 1 2 4 0 0.5 1 2 4 0 0.5 1 2 4
GLI2FL
GLI3FL
GLI3R
α-tubulin
Lamin A

Figure S4, related to Figure 5 and Figure 6. EFCAB7 and IQCE are positive regulators of the Hh signaling.

(A) Hh reporter activity (mean±SD, n=3) measured ± SAG treatment (24 h) in NIH/3T3 cells depleted of IQCE, EFCAB7, SMO or GLI2, with the latter two controls being known positive regulators of Hh signaling. Statistical significance was established using an unpaired student's t-test; $p<0.05$ (*). (B) Effect of IQCE and EFCAB7 depletion on the frequency of ciliation in NIH/3T3 cells. The mean (±SD) percentage of ciliated cells is shown derived from three independent experiments with n=100 in each experiment. (C) SAG-induced (24 h) GLI1 induction is diminished in C3H10T1/2 cells by the depletion of IQCE with a siRNA directed against the 3'-UTR in the native transcript. Stable reintroduction of a cDNA encoding HA-tagged IQCE but lacking this 3'-UTR confers resistance to the siRNA, demonstrating an on-target effect. GAPDH served as the loading control. (D) Hh reporter activity in response to a 24 h exposure to Shh conditioned media (CM, 1:20 dilution), SAG (100 nM), or 20(S)-hydroxycholesterol (10 μM) in wild-type NIH/3T3 cells, *Efcab7*$^{-/-}$ cells, or *Efcab7*$^{-/-}$ cells rescued with transient expression of YFP-EFCAB7. Mean (±SD, n=3) reporter activity is plotted, with significance tested using an unpaired student's t-test; $p<0.05$ (*) and $p<0.01$ (**). (E) Length of cilia in *Efcab7*$^{-/-}$ or *Efcab7*$^{-/-}$ cells transfected with YFP-EFCAB7. Each dot denotes the length of a single cilium, with the red brackets showing the median length with interquartile range calculated from 50 cilia. Significance test: Mann-Whitney test; $p>0.05$ (ns). (F) The mean (±SD, three experiments with n=100 cilia per experiment) frequency of ciliation is not affected by the loss of EFCAB7. (G) EFCAB7 loss in NIH/3T3 cells does not change the localization of a distal centrosome protein (CEP164) or a ciliary small GTPase (ARL13B). These ciliary proteins are in green and cilia are marked in red (anti-acTub). Scale bar: 2 μm. (H) Accumulation of endogenous SMO in cilia after 4 h of SAG treatment in *Efcab7*$^{-/-}$ or *Efcab7*$^{-/-}$ cells transiently transfected with YFP-EFCAB7. (I) Accumulation of endogenous GLI2 in the nucleus of cells with or without EFCAB7 in response to SAG (4 h). In H and I, each point represents a single cell and

red brackets show the median length with interquartile ranges derived from measurements from multiple cilia (n=50 for SMO and n=100 for GLI2); significance was tested using the Kruskal-Wallis test with $p>0.05$ (ns) and $p<0.0001$ (****). (J) Subcellular fractionation was used to determine the amounts of endogenous full-length GLI2 (GLI2FL), full-length GLI3 (GLI3FL) or the repressor fragment of GLI3 (GLI3R) in the nucleus and cytoplasm of cells at various time points after treatment with SAG. α-tubulin and Lamin A levels served as loading controls for the cytoplasmic and nuclear fractions, respectively, and also established the quality of the fractionation.

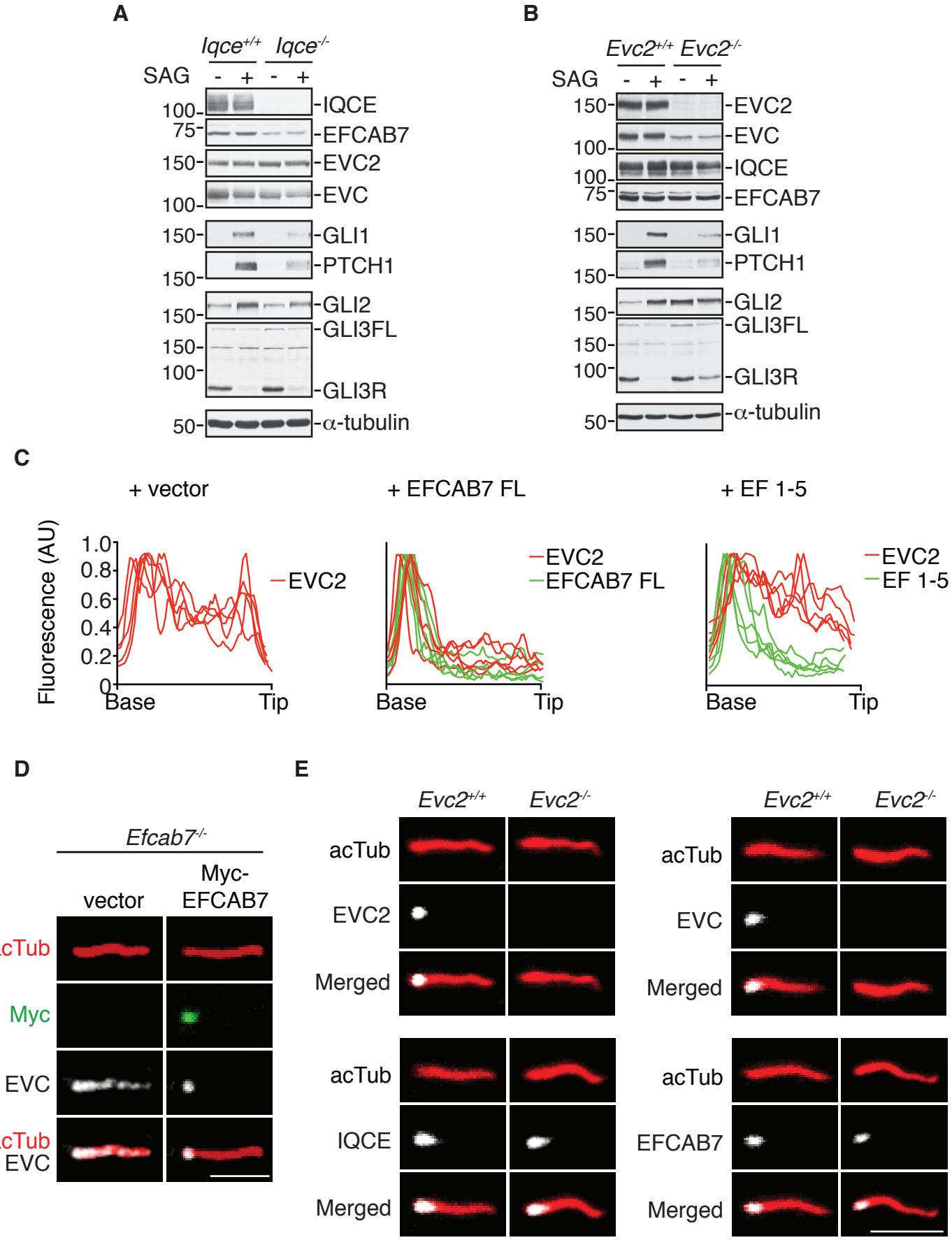
A
Iqce+/+
Iqce-/-
SAG - + - +
100
75
IQCE
EFCAB7
150
EVC2
100
EVC
150
GLI1
PTCH1
150
150
GLI2
150
GLI3FL
150
100
GLI3R
50
α-tubulin
B
Evc2+/+
Evc2-/-
SAG - + - +
150
EVC2
100
EVC
100
IQCE
75
EFCAB7
150
GLI1
PTCH1
150
150
GLI2
150
GLI3FL
150
100
GLI3R
50
α-tubulin
C
+ vector
+ EFCAB7 FL
+ EF 1-5
Fluorescence (AU)
1.0
0.8
0.6
0.4
0.2
0
EVC2
Base
Tip
EVC2
EFCAB7 FL
Base
Tip
EVC2
EF 1-5
Base
Tip
D
Efcab7-/-
vector
Myc-EFCAB7
acTub
Myc
EVC
acTub
EVC
E
Evc2+/+
Evc2-/-
acTub
EVC2
Merged
acTub
IQCE
Merged
Evc2+/+
Evc2-/-
acTub
EVC
Merged
acTub
EFCAB7
Merged

Figure S5, related to Figure 6. Characterization of Hh signaling and EvC complex localization in *Iqce*$^{-/-}$, *Evc2*$^{-/-}$, and *Efcab7*$^{-/-}$ cells.

(A) Immunoblots of extracts from *Iqce*$^{+/+}$ and *Iqce*$^{-/-}$ cells treated ± SAG (24 h) were used to assess levels of the indicated EvC complex and Hh pathway components. α-tubulin served as the loading control, GLI1 and PTCH1 are known Hh target genes, and GLI3FL and GLI3R point to the full-length GLI3 and its repressor fragment, respectively. (B) Immunoblots of extracts from *Evc2*$^{+/+}$ and *Evc2*$^{-/-}$ cells treated ± SAG (24 h) analyzed as in (A). (C) Normalized line scans of EVC2 fluorescence (red) along the lengths of five cilia from *Efcab7*$^{-/-}$ cells transiently transfected with a control vector (left), full-length EFCAB7 (middle) or the EF1-5 fragment of EFCAB7 (right). In the latter two cases, the EFCAB7 fluorescence along the cilium is shown in green. (D) Localization of endogenous EVC (white) in *Efcab7*$^{-/-}$ cells or *Efcab7*$^{-/-}$ cells transfected with Myc-tagged full-length EFCAB7 (green). Cilia (red) are oriented with their base to the left and tip to the right. (E) Localization of endogenous EVC2, EVC, IQCE, and EFCAB7 (white) within individual cilia, identified by axonemal anti-acetylated tubulin staining (acTub, red) and oriented with the base at the left and tip at the right in *Evc2*$^{+/+}$ or *Evc2*$^{-/-}$ cells. Scale bars are 2 μm in all images.

Figure S6

	IQCE	EFCAB7	EVC	EVC2	EVC3.1	EVC3.2	Hedgehog signaling	Primary cilia/ equivalent
Salpingoeca rosetta (Choanoflagellida)	+	+	-	-	+	+	HINT/ Hedgeling	+
Amphimedon queenslandica	-	-	-	-	-	-	HINT/ Hedgeling	+
Trichoplax adhaerens	+	+	+	+	+	+	-	+
Nematostella vectensis	-	+	+	+	+	+	HINT/ Hedgeling/ Hedgehog	+
Hydra magnipapillata	+	+	-	-	+	+	HINT/ Hedgeling/ Hedgehog	+
Caenorhabditis elegans	-	-	-	-	-	-	Multiple HINTs	Sensory neurons only
Drosophila melanogaster	-	-	-	-	-	-	Hedgehog	Sensory neurons + Spermatozoa
Danio rerio	+	+	- (Pseudogene)	-	+	+	Hedgehog	+
Homo sapiens	+	+	+	+	- (Pseudogene)	- (Pseudogene)	Hedgehog	+

Figure S6, related to Figure 7. Phylogenetic distribution of EvC complex components in comparison with the presence of Hedgehog signaling components and the presence of primary cilia.

The presence and absence of a component in the indicated species is marked by "+" and "-" respectively.

Supplemental Experimental Procedures

Constructs

All EvC complex constructs used the mouse sequence. Constructs encoding EVC, EVC2, EVC2ΔW (a.a. 1-1176), and SMO-M2 were described previously (Dorn et al., 2012). For this study, mouse EVC was also cloned with an N-terminal 3xHA tag. Full-length IQCE and EFCAB7 (or fragments thereof) were cloned with N-terminal YFP, 3xHA tag, or 6xMyc tags. pCS2+ or pCS-DEST (Addgene 22423) vectors were used for *in vitro* translation or transient expression in mammalian cells, pEF5/FRT/V5-DEST (Life Technologies) for transient mammalian expression or the construction of stable Flp-In cell lines, pLENTI CMV Puro DEST (Addgene 17452) for lentiviral production and pGex-FA vector (GE Life Sciences) or pMal-FA (New England Biolabs) for bacterial production of recombinant protein. Mutations were introduced by inverse PCR or the QuikChange method (Agilent) to generate N-terminal tagged versions of IQCE 1-139 (a.a. 1-139), IQCE 1-351 (a.a. 1-351), IQCE 1-489 (a.a. 1-489), IQCE 1-552 (ΔIQ-IQCE; a.a. 1-552), IQCE ΔN (a.a. 1-139 deleted), IQCE ΔCC1 core (a.a. 142-211 deleted), IQCE ΔCC1 (a.a. 140-351 deleted), IQCE ΔCC2 (a.a. 362-489 deleted), IQCE Δ3x IQ (a.a. 530-635 deleted), IQCE ΔAcidE (a.a. 749-778 deleted), EFCAB7 EF 1-5 (a.a. 1-248), EFCAB7 ECH1 (a.a. 249-396), EFCAB7 EF 6-8 (a.a. 400-540), EFCAB7 ECH2 (a.a. 540-628), $EVC2W^{WT}$ (a.a. 1133-1220), and $EVC2W^{Ala}$ (a.a. 1133-1220 with mutations in FVFR motif)

Reagents and Antibodies

n-Dodecyl-β-D-Maltopyranoside (DDM) and cholesteryl hemisuccinate (CHS) were purchased from Affymetrix, Dynabeads M-270 carboxylic acid and Protein A/G beads from Life Technologies, SAG from Enzo Life Sciences, and FLAG peptide from Sigma. Rabbit polyclonal antibodies against EVC, EVC2, SUFU, SMO, PTCH1 have been described previously (Dorn et

al., 2012; Rohatgi et al., 2007). Rabbit polyclonal antibodies against the N-terminal (1-166) and C-terminal (637-778) domains of mouse IQCE and full-length mouse EFCAB7 were generated in rabbits (Cocalico Biologicals) and affinity purified prior to use. Rabbit polyclonal antibodies against ARL13B and CEP164 have been described previously (Dorn et al., 2012; Graser et al., 2007). Commercially available antibodies used in this study include polyclonal antibodies against GFP (for IF: Rockland; for IB: Novus), GST (Bethyl), Myc (for IF: Bethyl), GLI2 (R&D), GLI3 (R&D), PKA (BD), Lamin A (Abcam), and monoclonal antibodies against HA (Covance), Myc (for IB: Roche), GLI1 (Cell Signaling), GAPDH (Abcam), acetylated-tubulin, α-tubulin, and FLAG (Sigma). Secondary antibodies conjugated to horseradish peroxidase or Alexa Fluor dyes were obtained from Jackson Laboratories and Molecular Probes, respectively.

Cell Lines

NIH/3T3, C3H10T1/2 and HEK293T cells were obtained from ATCC and Flp-In NIH/3T3 cells for stable cell lines construction from Life Technologies. Stable cell lines expressing tagged EVC, EVC2, EFCAB7 and IQCE (or their mutants) were produced by site-specific recombination into a single site in the genome using the Flp-In system (Life Technologies). Cell lines were cultured in DMEM (Thermo Scientific) supplemented with 10% fetal bovine serum (FBS), 1 mM sodium pyruvate, 2 mM L-Glutamine, 1x MEM non-essential amino acids solution (Gibco), penicillin (40 U/ml) and streptomycin (40 µg/ml), in a humidified atmosphere containing 5% CO_2 at 37 °C. NIH/3T3 and C3H10T1/2 cells were transfected with X-tremeGENE 9 (Roche), and HEK 293T cells were transfected with polyethylenimine (Polysciences). Stable C3H10T1/2 cells expressing siRNA-resistant IQCE was made using lentiviral infection with pLENTI CMV Puro DEST (Addgene 17452) vector and selection with puromycin (2μg/ml).

siRNA methods

MISSION siRNA universal negative control, si *Smo* (SASI_ Mm_02_00346929), and si *Evc2* (SASI_Mm01_00106977) were obtained from Sigma, si *Iqce* pool (M-059692-01-0005), si *Efcab7* pool (M-051995-00-003), si *Efcab7*_1 (D-051995-02), si *Efcab7*_2 (D-051995-04), and si *Gli2* (J-043977-10) were obtained from Thermo Scientific Dharmacon. si *Iqce*_1 (SI01077237) was obtained from Qiagen. NIH/3T3 and C3H10T1/2 cells were transfected with 25 nM siRNA using Lipofectamine RNAiMAX (Invitrogen) according to the manufacturer's instructions.

Hedgehog signaling assays

To induce ciliation (a requisite for Hh signaling), cells were grown to confluence in medium containing 10% FBS and then switched to medium containing 0.5 % FBS with pathway agonists for 24 h (unless indicated otherwise). In all cases SAG was used at 100 nM and Shh conditioned medium at a 1/20 dilution. For luciferase-based Hedgehog reporter assays (Sasaki et al., 1997), cells were transfected with a 4:1 w/w ratio of a firefly luciferase reporter driven by an 8xGli-responsive promoter and a Renilla luciferase reporter driven by a constitutive TK promoter (Promega), grown to confluence and then serum starved for 24 h with Hh agonists. Activity of both reporters was measured using the Dual-Luciferase Reporter kit (Promega) and read on a Synergy H1 Hybrid Multi-Mode Microplate Reader (BioTek). The Gli luciferase to Renilla luciferase ratio is reported as "Hedgehog reporter activity." To measure alkaline phosphatase expression, C3H10T1/2 cells were transfected with the indicated siRNAs, grown to confluency, and treated with SAG (100 nM) for 36 h in 0.5% FBS containing DMEM. After lysis (100 mM Tris pH 9.4, 250 mM NaCl, 25 mM $MgCl_2$, 1% [v/v] Triton-X100), alkaline phosphatase activity was measured using the CDP-Star Chemiluminescence reagent (Perkin Elmer).

Tandem affinity purification and Mass spectrometry

One hundred 15 cm plates of NIH/3T3 cells stably expressing EVC2-YFP-FLAG were serum starved for 24 h and then treated with 100 nM SAG for 2 h. Cells were washed twice with ice-

cold PBS followed by 10 mM HEPES pH 7.4 and swollen in the same hypotonic buffer for 10 min. The buffer was removed carefully and cells were scraped with SEAT buffer (10 mM triethanolamine/acetic acid, 1 mM EDTA pH 8.0, 250 mM sucrose, protease inhibitor cocktail) to a final volume of 100 ml and homogenized with twenty strokes of a dounce homogenizer. The sample was spun at 900xg for 8 min to collect the post-nuclear supernatant (PNS). The PNS was spun at 142,000xg for 60 min at 4 °C to harvest a membrane pellet, which was then resuspended by douncing in a membrane extraction buffer (MEB) containing 50 mM Tris-HCl pH-7.4, 150 mM NaCl, 1% DDM, 0.1% CHS, 1 mM $MgCl_2$, 1 mM EDTA, 1 mM EGTA, 0.2 mM DTT, 10% glycerol, 1 mM NaF, 1 mM Na_3VO_4, 1 µM microcystin-LR, and 1x protease inhibitor cocktail. After incubation for 1h at 4°C, the detergent extract was clarified by centrifugation at 140,000xg for 60 min at 4°C and then incubated with Anti-FLAG-M2 conjugated agarose beads (Sigma) for 16 h at 4°C. Beads were washed once with MEB followed by a single wash each in wash buffer A (MEB containing 0.1% DDM, 0.1% CHS, and 300 mM NaCl) and wash buffer B (MEB containing 0.1% DDM, 0.1% CHS). Bound protein complexes were eluted with 0.2 mg/ml FLAG peptide (Sigma) for 4 h at 4°C followed by an additional round of elution at 22°C for 1 h. The eluates were pooled and subjected to a second round of immunoprecipitation with GFP binding protein (GBP) covalently conjugated to carboxylic acid decorated Dynabeads M-270 for 2 h at 4°C. GBP beads were washed five times with buffer B and the bound complexes were eluted in 5x Laemmli buffer at 37°C for 30 min. The eluted sample was subjected to SDS-PAGE on a 8% Tris-Glycine gel followed by GelCode Blue staining (Thermo Scientific) to visualize protein bands. Protein bands were excised, digested with trypsin and analyzed (MS Bioworks) using a nano LC/MS/MS with a NanoAcquity HPLC system (Waters) interfaced to an Orbitrap Velos Pro (Thermo Scientific). The data were processed with the Mascot Server (Matrix Science) and the Mascot DAT files were parsed into the Scaffold software for validation, filtering and to create a non-redundant list per sample. Data were filtered using a minimum protein value

of 90%, a minimum peptide value of 50% (Prophet scores) and requiring at least two unique peptides per protein.

Immunoprecipitation and Western Blotting

Whole cell extracts from NIH/3T3 cells were prepared in a lysis buffer containing 50 mM Tris-HCl pH-8.0, 150 mM NaCl, 1% DDM, 0.1% CHS, 1 mM $MgCl_2$, 1 mM DTT, 10% Glycerol, 1x EDTA-free protease inhibitor cocktail (Sigma). Clarified supernatants were pre-cleared with Dynabeads alone (Life Technologies) for 30 min at 4 °C, followed by incubation with antibody-coupled Dynabeads for 2 h at 4 °C. Immobilized proteins were washed twice with lysis buffer followed by a wash with buffer A (lysis buffer with 0.1% DDM, 0.01% CHS, and 300 mM NaCl) and buffer B (lysis buffer with 0.1% DDM, 0.01% CHS). Samples were resuspended in Laemmli buffer and subjected to SDS-PAGE followed by Western blotting. Immunoprecipitations from HEK 293T cells were performed as described above except that the lysis buffer and wash buffers were the same (50 mM Tris-HCl pH-7.4, 150 mM NaCl, 1% NP-40, 1 mM EDTA, 1 mM EGTA, 1 mM DTT, 10% glycerol, 1 mM NaF and 1x EDTA-free protease inhibitor cocktail). For quantification of bands on western blots, films were scanned using the Epson Perfection V700 Photo scanner at 600 d.p.i as grayscale TIFF files and then opened in Image J.

Gel-filtration of detergent extracts from NIH/3T3 membranes

Post-nuclear supernatant (PNS) from ten 15 cm confluent, serum-starved NIH/3T3 cells was spun at 100,000xg for 1 h at 4 °C to isolate membranes. The membrane pellet was solubilized in a buffer containing 1x Phosphate Buffered Saline (PBS) pH-7.7, 1 mM $MgCl_2$, 1 mM DTT, 5% w/v glycerol, 2% DDM, 0.2% CHS, benzonase (10U/ml), and 1x protease inhibitor cocktail, for 1 h at 4°C with frequent dispersion of membranes with a pipette tip. EDTA was added to a final concentration of 1 mM and the sample was spun at 95,000xg for 1 h at 4 °C. The supernatant (2 mg of detergent solubilized membrane extract) was loaded on a Superose 6 10/300 GL FPLC

column (GE Healthcare) equilibrated and developed in buffer C (50 mM Tris-HCl pH 7.4, 150 mM NaCl, 5% glycerol, 1 mM DTT, 0.05% DDM and 0.005% CHS); 0.5 ml fractions were collected for analysis. Band intensities were calculated as described earlier and plotted as fraction of the total intensity in all analyzed fractions to determine elution profiles.

Glycerol gradient sedimentation analysis of detergent extracts from NIH/3T3 membranes

Post-nuclear supernatant (PNS) from ten 15 cm confluent, serum-starved NIH/3T3 cells was spun at 100,000xg for 1 h at 4 °C to isolate membranes. The membrane pellet was solubilized in a buffer containing 1x Phosphate Buffered Saline (PBS) pH-7.7, 1 mM $MgCl_2$, 1 mM DTT, 5% w/v glycerol, 2% DDM, 0.2% CHS, benzonase (10U/ml), and 1x protease inhibitor cocktail, for 1 h at 4°C with frequent dispersion of membranes with a pipette tip. EDTA was added to a final concentration of 1 mM and the sample was spun at 95,000xg for 1 h at 4 °C. The supernatant (2 mg of detergent solubilized membrane extract) was loaded on a 12 ml 10%-30% w/w glycerol gradient poured in buffer C (50 mM Tris-HCl pH 7.4, 150 mM NaCl, 5% glycerol, 1 mM DTT, 0.05% DDM and 0.005% CHS) using a Biocomp Gradient Master. Gradients were spun at 234,116x*g* in a SW41 rotor for 16 h at 4°C with slow acceleration and no brake. Fractions (0.5 ml each) were collected from the top for analysis. Band intensities were calculated as described earlier and plotted as fraction of the total intensity in all analyzed fractions to determine elution profiles.

Microscopy and image analysis

Immunofluorescence (IF) staining was performed as described previously (Dorn et al., 2012), except for Gli2 staining in the cytoplasm and nucleus (Figure 5F) where the blocking buffer contained 2% donkey serum and 0.2% Triton X-100 in PBS. Images were acquired on an inverted Leica SP8 confocal microscope with a 63X oil immersion objective (NA 1.4); 7X zoom was used for imaging of individual cilia. Z-stacks were acquired with identical acquisition

settings (gain, offset, laser power, frame format) within a given experiment and all measurements of fluorescence intensity were performed on maximum intensity projections in ImageJ. The fluorescence intensities of EVC2, EVC, IQCE and EFCAB7 at the base of cilia, SMO in the entire cilia, and GLI2 at the ciliary tips were measured as described previously (Dorn et al., 2012). For the quantification of SMO at cilia, a mask was constructed based on the acetylated tubulin image and then applied to the corresponding SMO image to measure the fluorescence intensity of SMO at cilia. To determine the ratio of nuclear to cytoplasmic fluorescence intensity of GLI2, nuclear fluorescence (guided by the DAPI signal) was measured and subtracted from total cell fluorescence to yield cytoplasmic GLI2 fluorescence intensity.

To determine the co-localization of EVC, EVC2, and IQCE with acetylated tubulin in Figure 6, the ImageJ plugin JACoP (Bolte and Cordelieres, 2006) was used to threshold the images and calculate the overlap of acetylated tubulin with EVC, EVC2, and IQCE (Mander's M2 coefficient). The fluorescence intensity traces of EVC2 and acetylated tubulin in Figure S5C were calculated in ImageJ by measuring the fluorescence intensity over the length of cilia and represented as fraction of maximum fluorescence.

For cilia length, a mask was constructed by applying a threshold to the acetylated tubulin image, followed by measurement of the area of each cilium in the image. Cilia frequency measurements were done by manually counting the fraction of DAPI-positive cells that were positive for acetylated tubulin-marked cilia.

Recombinant protein expression and purification

Single colonies of *Escherichia coli* (BL21 strain) transformed with PGEX plasmids encoding GST-EVC2W^{WT} and GST-EVC2W^{Ala} were inoculated into 50 ml LB medium containing 100 µg/ml carbenicillin and cultured overnight at 37°C. 2 L of fresh LB medium was inoculated (2% from overnight cultures) and grown at 37°C to an A_{600} = 0.5. The cells were induced with 1 mM isopropyl-β-D-thiogalactopyranoside and grown for an additional 4 h at 22°C. Bacteria were

pelleted and stored at -80°C. Frozen pellets were quickly thawed in a water bath at 37°C and resuspended in lysis buffer (50 mM Tris-HCl pH 8.0, 150 mM NaCl, 2 mM $MgCl_2$, 1 mM DTT) supplemented with protease inhibitor cocktail and lysed by two passages through an EmulsiFlex-C5 at 20,000 p.s.i. (Avestin). Lysates were clarified by centrifugation at 48,000x*g* for 30 min at 4°C. Clarified samples were filtered through a 0.45 µm filter and incubated with 1 ml of packed glutathione sepharose 4B beads (GE Healthcare) for 3 h at 4°C. The resin was washed with 20 column volumes of lysis buffer and bound proteins eluted in a buffer containing 50 mM Tris-HCl pH 8.0, 150 mM NaCl, 1 mM DTT, 20 mM reduced glutathione. Fractions were pooled, dialyzed against storage buffer (50 mM Tris-HCl pH 8.0, 150 mM NaCl, 1 mM DTT, and 10% glycerol) and stored at -80 °C. The recombinant protein was >95% pure, as assessed from coomassie staining.

***In vitro* binding assays**

For GST pulldown assays, 10 µg of purified GST-EVC2W^{WT} and GST-EVC2W^{Ala} were immobilized on glutathione sepharose 4B beads and tested for their ability to pull-down IQCE and EFCAB7 expressed using the TNT coupled wheat germ extract system (Promega). For interactions between EFCAB7 and IQCE, protein fragments whose interaction was being tested were *in vitro* translated together, followed by immunoprecipitation of one of the fragments.

IQCE and EFCAB7 were expressed using the TNT coupled wheat germ extract system (Promega) and incubated with these beads in buffer D (50 mM Tris-HCl pH-8.0, 150 mM NaCl, 0.5% NP40, 1 mM $MgCl_2$, 1 mM EDTA, 1 mM EGTA, 1 mM DTT, 10% glycerol, 0.5 mg/ml chicken egg albumin, and 1x protease inhibitor cocktail) for 2 h at 4°C. Beads were five times with buffer D without chicken egg albumin and samples were eluted in 2X Laemmli buffer for analysis by immunoblotting.

For the binding assay in Figure 4 between EFCAB7 and IQCE, protein fragments whose interaction was being tested were *in vitro* translated together and then incubated with GBP-

coupled Dynabeads in buffer E (20 mM HEPES pH 7.7, 150 mM NaCl, 0.1% NP-40, 1 mM $MgCl_2$, 0.1 mM EDTA, 1 mM DTT, 0.5 mg/ml chicken egg albumin, 10% glycerol, and 1x protease inhibitor cocktail) for 2 h at 4 °C. Beads were washed once each with buffer E, buffer E with 0.5% NP-40, buffer E with 500 mM NaCl, and buffer E without NaCl. Samples were eluted in 2X Laemmli buffer for analysis by immunoblotting

Real-time, reverse-transcription PCR (qRT-PCR)

Total cell RNA was extracted using TRIzol reagent (Life Technologies) and cDNA was synthesized using iScript Reverse Transcription Supermix for RT-qPCR (Biorad) following the manufacturer's instructions. Quantitative, reverse-transcription PCR (qRT-PCR) was performed with a 7900HT Fast Real-Time PCR System (Applied Biosystems) using the iTaq SYBR Green Supermix with ROX (Biorad) and custom designed primers for *Gli1* (forward primer: 5'-ccaagccaactttatgtcaggg-3' and reverse primer: 5'-agcccgcttctttgttaatttga-3'), *Iqce* (forward primer: 5'-aagagaacccaacacaagagg-3' and reverse primer: 5'-cagatcctgagggtgtcaatg-3'), *Efcab7* (forward primer: 5'-gcaatggtctgattagccttg-3' and reverse primer: 5'-agtccataaagccctgtcttg-3'), and *Gapdh* (forward primer: 5'-ggccttccgtgttcctac-3' and reverse primer: 5'-tgtcatcatacttggcaggtt -3'). Transcript levels relative to *gapdh* were calculated using the ΔΔCt method.

Generation of NIH/3T3 cell lines carrying null mutations in EvC complex subunits

Efcab7$^{-/-}$, *Evc2*$^{-/-}$ and *Iqce*$^{-/-}$ cells were generated using the CRIPSR/Cas9 genome editing strategy using Addgene plasmid number 42230 and the guide sequences 5'-aactgaggcgtcaacagtt-3' (*Efcab7*), 5'-gatatttcaaaaatgctcac-3' (*Evc2*), 5'-ggcgatctctgaagacggca-3' (*Iqce*). (Cong et al., 2013). The targeting CRISPR plasmid was co-transfected with a YFP-containing plasmid using X-tremeGENE 9 and single cells expressing YFP were sorted into 96 well plates using FACSAria II (BD). Single clones that had lost expression of the targeted

protein were identified using immunoblotting. The frequencies at which NIH/3T3 clones bearing null mutations in both alleles of *Efcab7, Iqce*, and *Evc2* were retrieved were 5%, 1% and 5% respectively.

Protein sequence analysis, domain identification and phylogenetic analysis.

Iterative sequence profile searches were performed using the PSI-BLAST program run against the NCBI non-redundant (NR) protein database (Altschul et al., 1997). Multiple sequence alignments were built by the Kalign2 (Lassmann et al., 2009) and Muscle (Edgar, 2004) programs, followed by manual adjustments on the basis of profile-profile, secondary structure information and structural alignments. Similarity-based clustering for both classification and culling of nearly identical sequences was performed using the BLASTCLUST program (ftp://ftp.ncbi.nih.gov/blast/documents/blastclust.html). The HHpred program was used for profile–profile comparisons (Soding et al., 2005). Secondary structures were predicted using the JPred program (Cuff et al., 1998). For previously characterized domains, the PFAM database was used as a guide (Punta et al., 2012). Clustering with BLASTCLUST followed by multiple sequence alignment and further sequence profile searches were used to identify novel domains that were not present in the PFAM database. Structural visualization and manipulations were performed using the PyMol program (http://www.pymol.org). Phylogenetic trees were constructed using FastTree 2.1 which implements an approximately maximum-likelihood method (Price et al., 2009), and rendered using MEGA4 (Tamura et al., 2007) and FigTree (http://tree.bio.ed.ac.uk/software/figtree/) programs.

Sequence analysis of the extracellular globular domain in EVC2

Searches using this globular domain with the HHpred program against a panel of Hidden Markov models built from domains in the PDB database recovered significant hits to sugar-binding β-sandwich domains (e.g. those from β-galactosidase; $p=10^{-5}$-10^{-7}; probability= 75-

90%). This was consistent with its predicted secondary structure and showed that this domain of EVC2 is likely to adopt a β-sandwich fold that may contact ligands in the extracellular space.

Sequence analysis of the ECH1 and ECH2 domains in EFCAB7

To better understand the two uncharacterized globular domains in EFCAB7 we ran sequence profile searches with them using the PSI-BLAST program. The first of these globular domains is related to a conserved globular domain observed in several calpains such as the μ-calpains. In calpains, this domain also occurs immediately after an EF-hand domain and has been termed region-III. Accordingly we named it the EFCAB7-calpain homology 1 (ECH1) domain (Figure 4A and Figure S2). While there is conflicting data on membrane binding of this globular domain in μ-calpains (Fernandez-Montalvan et al., 2006; Tompa et al., 2001), it is possible that the ECH1 β-sandwich in EFCAB7 plays a role in membrane contact. The C-terminal globular domain of EFCAB7 was also found to be shared with a specific group of calpains, the calpain-15/Small optic lobes group but not with other calpains, and thus we named it the ECH2 (EFCAB7-Calpain-homology 2) domain (Figure 4A and Figure S2). Profile-profile comparisons recovered β-sandwich domains from amylases (e.g. PDB: 4E2O; $P=10^{-14}$; Probability=92%) suggesting that ECH2, like ECH1, adopts a β-sandwich fold.

Phylogenetic analysis of EVC and EVC2 (Figure 7)

As coiled-coil regions can skew sequence searches and increase the rate of false positives, we built sequence profiles with low inclusion e-values ($e<10^{-12}$) to identify new potential homologs of EVC and EVC2 and then tested these candidates for reciprocal preferential recovery of EVC and EVC2.

Statistical analysis

Statistical analysis for fluorescence intensity comparisons between two or multiple groups was performed by Mann-Whitney test or the Kruskal-Wallis non-parametric ANOVA test,

respectively. The statistical significance between the means in Hh reporter assays was determined by a two-tailed, unpaired Student's *t* test.

Supplemental References

Altschul, S.F., Madden, T.L., Schaffer, A.A., Zhang, J., Zhang, Z., Miller, W., and Lipman, D.J. (1997). Gapped BLAST and PSI-BLAST: a new generation of protein database search programs. Nucleic acids research *25*, 3389-3402.

Bolte, S., and Cordelieres, F.P. (2006). A guided tour into subcellular colocalization analysis in light microscopy. Journal of microscopy *224*, 213-232.

Cong, L., Ran, F.A., Cox, D., Lin, S., Barretto, R., Habib, N., Hsu, P.D., Wu, X., Jiang, W., Marraffini, L.A.*, et al.* (2013). Multiplex genome engineering using CRISPR/Cas systems. Science *339*, 819-823.

Cuff, J.A., Clamp, M.E., Siddiqui, A.S., Finlay, M., and Barton, G.J. (1998). JPred: a consensus secondary structure prediction server. Bioinformatics *14*, 892-893.

Dorn, K.V., Hughes, C.E., and Rohatgi, R. (2012). A Smoothened-Evc2 complex transduces the Hedgehog signal at primary cilia. Dev Cell *23*, 823-835.

Edgar, R.C. (2004). MUSCLE: multiple sequence alignment with high accuracy and high throughput. Nucleic acids research *32*, 1792-1797.

Fernandez-Montalvan, A., Assfalg-Machleidt, I., Pfeiler, D., Fritz, H., Jochum, M., and Machleidt, W. (2006). Mu-calpain binds to lipid bilayers via the exposed hydrophobic surface of its Ca2+-activated conformation. Biological chemistry *387*, 617-627.

Graser, S., Stierhof, Y.D., Lavoie, S.B., Gassner, O.S., Lamla, S., Le Clech, M., and Nigg, E.A. (2007). Cep164, a novel centriole appendage protein required for primary cilium formation. J Cell Biol *179*, 321-330.

Lassmann, T., Frings, O., and Sonnhammer, E.L. (2009). Kalign2: high-performance multiple alignment of protein and nucleotide sequences allowing external features. Nucleic acids research *37*, 858-865.

Price, M.N., Dehal, P.S., and Arkin, A.P. (2009). FastTree: computing large minimum evolution trees with profiles instead of a distance matrix. Molecular biology and evolution *26*, 1641-1650.

Punta, M., Coggill, P.C., Eberhardt, R.Y., Mistry, J., Tate, J., Boursnell, C., Pang, N., Forslund, K., Ceric, G., Clements, J.*, et al.* (2012). The Pfam protein families database. Nucleic acids research *40*, D290-301.

Rohatgi, R., Milenkovic, L., and Scott, M.P. (2007). Patched1 regulates hedgehog signaling at the primary cilium. Science *317*, 372-376.

Sasaki, H., Hui, C., Nakafuku, M., and Kondoh, H. (1997). A binding site for Gli proteins is essential for HNF-3beta floor plate enhancer activity in transgenics and can respond to Shh in vitro. Development *124*, 1313-1322.

Soding, J., Biegert, A., and Lupas, A.N. (2005). The HHpred interactive server for protein homology detection and structure prediction. Nucleic acids research *33*, W244-248.

Tamura, K., Dudley, J., Nei, M., and Kumar, S. (2007). MEGA4: Molecular Evolutionary Genetics Analysis (MEGA) software version 4.0. Molecular biology and evolution *24*, 1596-1599.

Tompa, P., Emori, Y., Sorimachi, H., Suzuki, K., and Friedrich, P. (2001). Domain III of calpain is a ca2+-regulated phospholipid-binding domain. Biochem Biophys Res Commun *280*, 1333-1339.